

PMUs Clock De-Synchronization Compensation for Smart Grid State Estimation

Marco Todescato and Ruggero Carli and Luca Schenato and Grazia Barchi

Abstract—We address the problem of power system state estimation based on information coming from ubiquitous power demand time series and a limited number of PMUs. The presence of time synchronization error in the PMU measurements is explicitly considered. It is shown how incorrect modeling of synchronization errors easily lead to incorrect results, ruining the estimation performance of standard approaches. Resorting to a novel linear approximation for the power flow equations, we propose a Kalman based algorithm for the simultaneous estimation of system state and synchronization error parameters. Compelling numerical simulations, based on the IEEE C37.118.1 standard on PMUs, validate the proposed approach.

Index Terms—Power Systems State Estimation, Smart Grids, Time Synchronization, PMU, Kalman Filter.

I. INTRODUCTION

In recent years, the increasing penetration of variable energy and the transition from passive to active and non-linear loads, e.g. electrical-vehicle, have made monitoring and control operations of electric grids more challenging. Thus, in order to optimally plan and operate, a real-time knowledge of the system state is required at both the transmission and distribution level [1]. Because of different modeling assumptions and types of available information, till now, State Estimation (SE) at the transmission and distribution level has been addressed separately.

Extensive literature exists for transmission systems, mainly characterized by high line reactance/resistance (X/R) ratio, meshed topology and a large number of measurement points providing active and reactive power, voltage at buses and current flows along the branches [2]. Conversely, distribution systems, characterized by low X/R ratio, radial topology, unbalanced loads and a high number of nodes usually unmonitored, have traditionally lacked the situation awareness typically seen in transmission systems. However, increasing DER penetration has necessitated DSO's to improve system observability, usually in the form of SE [3]. In this context a central role is played by Phasor Measurement Units (PMUs) able to provide phasors of electrical waveforms synchronized with the Universal Coordinated Time (UTC) [4]. Initially conceived and applied at the transmission level, PMUs are gaining interest in distribution systems to support different applications among which SE is one of the most relevant. The availability of voltage magnitude and phase introduces

the possibility of directly measuring rather than estimating the state variables [5]. However, because of their high cost, only a limited number of PMUs is available, thus most of the recent solutions rely on measurements from a small number of PMUs along with conventional smart meter [6].

The high accurate PMU measurements, while improving SE, can be exploited for different operations but this requires an almost perfect synchronization with the UTC in order to avoid additional uncertainty contribution to phase angles. For this reason, in the literature most of works assume the PMUs perfectly synchronized and model additional uncertainty with a standard Gaussian distribution [6]. Conversely, different source of uncertainty are present in PMUs [7] with time synchronization representing one of them. Indeed, GPS provides 1pps (pulse-per-second) synchronization signals, with a theoretical accuracy of $1\mu s$ which affects synchronization offsets, while internal PMUs clocks present frequency deviations which can produce large time skews. In view of this, the SE problem in the presence of synchronization error has been studied in the more recent literature. In [8] a first investigation on the effect of sync error is provided together with a static distributed estimator suitable for distribution-only grids. In [9], by leveraging the assumption of small angle differences, the authors formulate a measurement model which is bilinear w.r.t. grid state and sync error parameters to which two parallel Kalman filters are applied. Finally, in [10] only PMUs offset error due to GPS is considered.

Inspired by the recent [6], we address the problem of SE based on PMU measurements and load pseudo-measurements. As opposed to [6], we explicitly consider the presence of synchronization error in the PMU measurements. The final aim is the simultaneous estimation of the system state as well as the time synchronization error which, if not correctly modeled can compromise the estimation performance of standard approaches.

The contributions are threefold: i) conversely to solutions in the literature, our methodology seamlessly applies to transmission and distribution grids since we base our analysis on a recently proposed generalized linear model for the power flow manifold [11]. ii) Since the prescribed approximation naturally expresses the voltages in polar coordinates, our measurement model is linear in the synchronization error parameters affecting the voltage phase angles. Hence, we propose a Kalman-based algorithm for the simultaneous estimation of the state and of the synchronization error parameters (offset and skew). iii) Based on the IEEE C37.118.1 [12] standard on PMUs, we practically quantify the extent to which modeling errors turn out to be totally misleading.

M.Todescato, R.Carli and L.Schenato are with the Dept. of Information Engineering of the University of Padova, via Gradenigo 6/B 35131 Padova, Italy. [todescat|carlirug|schenato]@dei.unipd.it. G.Barchi is with the Institute for Renewable Energy at EURAC Research, viale Druso 1 39100 Bolzano, Italy. Grazia.Barchi@eurac.edu.

II. POWER NETWORK MODEL

We envision a power network as a cyber-physical system consisting of a cybernetic layer and a physical layer. The cybernetic layer consists of a data aggregator (DA) and a Central Processing Unit (CPU). The DA is able to collect measurements coming from the smart metering devices the physical layer is equipped with. The CPU is in charge of all the computational payload and, in particular, of the SE algorithm. Regarding the physical layer, we assume each electric bus equipped with a low-cost smart meter which provides low-accuracy power measurements. Moreover, only some nodes have attached a PMU able to provide highly-accurate measurements. We refer the reader to Section III for further details on the measurement models. In addition, following the notation in [11] we model an AC power network, assumed to be in synchronous sinusoidal steady-state regime, as a graph $\mathcal{G}(\mathcal{V}, \mathcal{E})$ where the nodes set $\mathcal{V} = \{1, \dots, n\}$ denotes the electric buses, while the edges set \mathcal{E} denote the set of electric branches between connected buses. For each bus $h \in \mathcal{V}$, we define the following quantities, related to its phasor representation:

- voltage $u_h = v_h e^{j\theta_h} \in \mathbb{C}$, $v_h = |u_h|$, $\theta_h = \angle u_h \in \mathbb{R}$;
- injected current $i_h \in \mathbb{C}$;
- absorbed power $s_h = p_h + jq_h \in \mathbb{C}$, where $p_h, q_h \in \mathbb{R}$ are the active and reactive components, respectively.

We define the *nodal admittance matrix* $Y \in \mathbb{C}^{n \times n}$ via its elements

$$Y_{hk} = \begin{cases} y_h^{sh} + \sum_{\ell \neq h} y_{h\ell} & \text{if } k = h \\ -y_{hk} & \text{otherwise} \end{cases}$$

where y_{hk} is the admittance of the electric line (h, k) connecting bus h with bus k , while y_h^{sh} is the shunt admittance (admittance to ground) at bus h .

By collecting all the nodal quantities into vectors $\mathbf{u} = [u_1, \dots, u_n]^T$, $\mathbf{i} = [i_1, \dots, i_n]^T$, $\mathbf{s} = [s_1, \dots, s_n]^T$ and thanks to Kirchhoff's law and the nodal power balance, it holds, denoting with $\overline{(\cdot)}$ the complex conjugate operator, that

$$\mathbf{i} = Y\mathbf{u}, \quad \mathbf{s} = \text{diag}(\mathbf{u})\bar{\mathbf{i}}.$$

Then, by combining the two equations, one gets

$$\mathbf{s} = \text{diag}(\mathbf{u})\overline{Y\mathbf{u}}, \quad (1)$$

which has to be satisfied by any feasible power flow.

According to [11], we define the power network state vector as $\boldsymbol{\xi} := [\mathbf{v}^T, \boldsymbol{\theta}^T, \mathbf{p}^T, \mathbf{q}^T]^T$ where $\mathbf{v}, \boldsymbol{\theta}, \mathbf{p}, \mathbf{q} \in \mathbb{R}^n$ are obtained stacking together the corresponding nodal quantities. By using rectangular coordinates, it is possible to rewrite (1) in implicit form as $F(\boldsymbol{\xi}) = 0$, where $F: \mathbb{R}^{4n} \mapsto \mathbb{R}^{2n}$ which, as stated in Lemma 1 of [11], implicitly defines the *power flow manifold*

$$\mathcal{M} = \{\boldsymbol{\xi} \mid F(\boldsymbol{\xi}) = 0\}.$$

This reformulation is interesting since it defines all the voltages and power injections that are compatible with the physics without assuming any a priori model for the network's buses such as the typical PQ, PV or slack buses.

A. Best Linear Approximant

In this section we recall Proposition 1 of [11] which, given a point $\boldsymbol{\xi}^* \in \mathcal{M}$, states how to reconstruct the best linear approximant, i.e., the plane tangent to \mathcal{M} at $\boldsymbol{\xi}^*$, of the power manifold \mathcal{M} at the feasible point $\boldsymbol{\xi}^*$.

Proposition 1 (Proposition 1 of [11]): Let $\boldsymbol{\xi}^* \in \mathcal{M}$, i.e., $\boldsymbol{\xi}^* = [(\mathbf{v}^*)^T, (\boldsymbol{\theta}^*)^T, (\mathbf{p}^*)^T, (\mathbf{q}^*)^T]^T$, such that $F(\boldsymbol{\xi}^*) = 0$. Then, the linear manifold tangent to \mathcal{M} in $\boldsymbol{\xi}^*$ is given by

$$A_{\boldsymbol{\xi}^*}(\boldsymbol{\xi} - \boldsymbol{\xi}^*) = 0, \quad (2)$$

where, being I the identity matrix of suitable size,

$$A_{\boldsymbol{\xi}^*} = \underbrace{\left[\langle \text{diag } \overline{Y\mathbf{u}^*} \rangle + \langle \text{diag } \mathbf{u}^* \rangle N \langle Y \rangle \right]}_{A_{\mathbf{u}^*}} R(\mathbf{u}^*) - I,$$

$$\mathbf{u}^* := \mathbf{v}^* e^{j\boldsymbol{\theta}^*}, \quad N := \begin{bmatrix} I & 0 \\ 0 & -I \end{bmatrix}, \quad \langle A \rangle = \begin{bmatrix} \text{Re } A & -\text{Im } A \\ \text{Im } A & \text{Re } A \end{bmatrix},$$

$$R(\mathbf{u}) := \begin{bmatrix} \text{diag}(\cos \boldsymbol{\theta}) & -\text{diag}(\mathbf{v})\text{diag}(\sin \boldsymbol{\theta}) \\ \text{diag}(\sin \boldsymbol{\theta}) & \text{diag}(\mathbf{v})\text{diag}(\cos \boldsymbol{\theta}) \end{bmatrix}. \quad \square$$

Assuming $A_{\mathbf{u}^*}$ invertible¹, the result of Proposition 1 states that it is possible to express the voltage deviations as linear functions of the power deviations, i.e.,

$$\begin{bmatrix} \delta \mathbf{v} \\ \delta \boldsymbol{\theta} \end{bmatrix} = A_{\mathbf{u}^*}^{-1} \begin{bmatrix} \delta \mathbf{p} \\ \delta \mathbf{q} \end{bmatrix}, \quad (3)$$

where $\delta \mathbf{v} := \mathbf{v} - \mathbf{v}^*$, $\delta \boldsymbol{\theta} := \boldsymbol{\theta} - \boldsymbol{\theta}^*$, $\delta \mathbf{p} := \mathbf{p} - \mathbf{p}^*$, $\delta \mathbf{q} := \mathbf{q} - \mathbf{q}^*$. The strength of the presented linear model is that it holds for any admissible working point $\boldsymbol{\xi}^* \in \mathcal{M}$. For instance, assuming absence of shunts, the flat profile $\boldsymbol{\xi}^* = [\mathbf{1}^T, 0^T, 0^T, 0^T]^T$ is feasible and corresponds to

$$A_{\boldsymbol{\xi}^*} = \begin{bmatrix} \text{Re } Y & -\text{Im } Y & -I & 0 \\ -\text{Im } Y & -\text{Re } Y & 0 & -I \end{bmatrix}$$

which equals the *Linear Coupled power flow* model [13]. Hence, (2) can be regarded as a generalization of many previously presented linear approximations. For the same reason, by assuming no a priori information on the particular physics of the grid, the liner approximant (3) seamlessly holds for distribution as well as for transmission grids.

III. MEASUREMENT MODELS

Our final goal is to simultaneously estimate the grid state, defined as the voltage magnitude \mathbf{v} and phase $\boldsymbol{\theta}$ at every bus of the network, and the synchronization error. To do so, in spirit of [6], we resort to two types of information: i) historical data series of active and reactive power demands; ii) real-time high-accuracy phasorial measurements.

A. Power Demand Time-Series

The first source of information are historical data series of power demands available from measurements collected at each bus from *low-cost largely-available* and, usually, *low accurate* smart meters. This source of information is affected by an uncertainty within 30% – 50% of the nominal values

¹The assumption is not restrictive since in real power grids and, in particular, in the presence of node shunt admittances, it is usually the case.

[14]. Therefore, the active and reactive power demands at node $h \in \mathcal{V}$ at time $t \in \mathbb{Z}_+$ are written as

$$\begin{aligned} \tilde{p}_h(t) &= p_h + w_h^p(t), & w_h^p(t) &\sim \mathcal{N}(0, \sigma_p^2 |p_h|^2), \\ \tilde{q}_h(t) &= q_h + w_h^q(t), & w_h^q(t) &\sim \mathcal{N}(0, \sigma_q^2 |q_h|^2), \end{aligned} \quad (4)$$

where p_h, q_h are the nominal values and where we assume $\sigma_p = \sigma_q \approx 30 - 50\%$ [14]. Moreover, in the following we assume uncorrelated noise [6], [14], that is $\mathbb{E}[w_k^p(t)w_k^q(t)] = \mathbb{E}[w_k^p(t)w_h^p(t)] = \mathbb{E}[w_k^q(t)w_h^q(t)] = 0$ for $h, k \in \mathcal{V}$, where $\mathbb{E}[\cdot]$ denotes the expectation operator.

B. PMU Measurements

The second source of information are phasor measurements coming from *high-cost highly accurate Phasor Measurement Units* which, because of their cost are deployed only at a limited number of electric buses. To provide highly accurate values, PMUs are equipped with a GPS module which is exploited for synchronization purposes. Hence, it is a common assumption to consider the PMUs as perfectly synchronized, thus neglecting the impact of synchronization uncertainty on the resulting measurements. Conversely, in this work we explicitly consider also the effect due to time clock synchronization error (de-synchronization).

More in details, the PMU measurements at a certain bus $h \in \mathcal{V}$ at time $t \in \mathbb{Z}_+$ are of the form

$$\begin{aligned} \tilde{v}_h(t) &= v_h(t) + w_h^v(t), & w_h^v(t) &\sim \mathcal{N}(0, \sigma_{\text{pmu},v}^2 |v_h|^2), \\ \tilde{\theta}_h(t) &= \theta_h(t) + w_h^\theta(t) + d_h(t), & w_h^\theta(t) &\sim \mathcal{N}(0, \sigma_{\text{pmu},\theta}^2), \end{aligned} \quad (5)$$

where $\sigma_{\text{pmu},v}$ and $\sigma_{\text{pmu},\theta}$ are the modulus and phase standard deviations. The synchrophasor reference Standard (i.e IEEE C37.118:2014a [12]) for PMUs suggests a Total Vector Error (TVE) below 1% in steady-state conditions. However, it is known that, especially at the distribution level, the accuracy required is higher due to the lower power flows and angle phase differences [15]. For this reason, we assume

$$\sigma_{\text{pmu},v} = 0.1\%, \quad \sigma_{\text{pmu},\theta} = 10^{-3}[\text{rad}]$$

As for the power demand measurements, also for PMU measurements, it is assumed the measurement noise to be uncorrelated within the same node and across different nodes, i.e., $\mathbb{E}[w_k^v(t)w_k^\theta(t)] = \mathbb{E}[w_k^v(t)w_h^v(t)] = \mathbb{E}[w_k^\theta(t)w_h^\theta(t)] = 0$ for $h, k \in \mathcal{V}$. Finally, the additional term $d_h(t)$, which models the time synchronization error or de-synchronization, represents the error with respect to the true universal time. Since this component mainly affects the angle measurements [7], we restrict our analysis to de-synchronization affecting the voltage angles only. In particular, we consider a clock error model which, within successive GPS synchronization time instants $kT, (k+1)T, \dots$, has the form

$$d_h(t) = \beta_h + \alpha_h \frac{T}{M} t, \quad t \in \mathbb{Z}[0, M],$$

where T is the GPS synchronization period, M is the number of PMU measurements collected within two successive synchronization instants; $\mathbb{Z}[0, M]$ denotes the subset of \mathbb{Z} from 0 to M ; β_h is an offset term due to GPS error which is

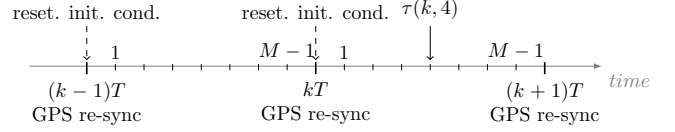


Fig. 1: Illustrative representation of the evolution of discrete time instants in a universal time frame with the GPS units re-synchronizing every T [s]. According to Algorithm 1, every T [s] initial conditions are initialized.

assumed constant in the time interval $[kT, (k+1)T)$; α_h is the clock skew due to the fact that the internal clock of the PMU, depending on the type of oscillator, might not oscillate at the reference frequency. As for the offset, the skew is assumed constant in the time interval $[kT, (k+1)T)$. Given the 1pps synchronization of GPS units, reasonable value is $T = 1$ s [9] while, for a 50Hz sinusoidal signal, we select a PMU reporting rate of 25Hz, thus $M = 25$ [12]. Finally, note that the assumption of constant α_h and β_h is reasonable conditioned to the relatively small synchronization period of $T = 1$ s. Observe that at each kT , offset β and skew α can assume both positive and negative values. For instance, a positive α means that the local clock frequency is faster than that of the universal time reference.

IV. ESTIMATION

As above mentioned, our final goal is: *to provide a good and almost real-time estimate* ($\hat{\mathbf{v}}, \hat{\boldsymbol{\theta}}, \hat{\boldsymbol{\alpha}}, \hat{\boldsymbol{\beta}}$) *of the system state* ($\mathbf{v}, \boldsymbol{\theta}$) *and of the PMUs de-synchronization parameters* ($\boldsymbol{\alpha}, \boldsymbol{\beta}$) *by leveraging the linear approximation (3) together with the information coming from ubiquitous power demand time series (4) and PMUs measurements (5).*

We cast our estimation procedure as a Bayesian inference process. More specifically, the idea is to exploit the power demand predictions, characterized by a low accuracy, to provide a prior for our Bayesian model. Then, high accuracy PMU measurements are used to improve the state estimate. Since our estimator consists of a Kalman filter [16], a state space model together with an output model are needed. Before outlining the models, observe that GPS re-synchronization instants and PMU measurements collection instants happen to live on two different time scales as shown in Figure 1. Hence, it is convenient to denote discrete instants in a universal time reference as

$$\tau(k, t) = kT + \frac{T}{M}t, \quad k \in \mathbb{Z}_+, \quad t \in \mathbb{Z}[0, M-1],$$

where k denotes the k -th re-synchronization instant while t the t -th PMU measurement. In the following, talking about the evolution of discrete-time systems, with a slight abuse of notation, instead of writing $\mathbf{x}(\tau(k, t))$ we write $\mathbf{x}(k, t)$.

A. State model

Given the linear relation (3) and the PMU measurement model (5), as inner state of the Kalman filter it is conve-

nient to pick the power demands deviations² $\delta\mathbf{p}, \delta\mathbf{q} \in \mathbb{R}^n$ together with the synchronization error parameters³ $\alpha, \beta \in \mathbb{R}^m$. Moreover, given $T = 1\text{s}$, within two consecutive re-synchronization instants, it is reasonable to assume a constant model for the power demands as already done for α and β . Hence, by defining the state vector

$$\mathbf{x}(k, t) := [\delta\mathbf{p}(k, t)^T \quad \delta\mathbf{q}(k, t)^T \quad \alpha(k, t)^T \quad \beta(k, t)^T]^T,$$

the state evolution reads as

$$\mathbf{x}(k, t+1) = \mathbf{x}(k, t), \quad \mathbf{x}(k, 0) \sim \mathcal{N}(0, P_0), \quad (6)$$

with $P_0 = \text{blkdiag}(\sigma_p^2 \text{diag}(|\mathbf{p}^*|^2), \sigma_q^2 \text{diag}(|\mathbf{q}^*|^2), \sigma_\alpha^2 I, \sigma_\beta^2 I)$ where blkdiag represent the block diagonal matrix made from its arguments and $\mathbf{p}^*, \mathbf{q}^*$ are the nominal/predicted values for active and reactive power demands available at $\tau(k, 0)$ computed using the time-series information. These are used as priors in our Bayesian model. Hence, the priors for $\delta\mathbf{p}$ and $\delta\mathbf{q}$ are equal to 0. $\sigma_\alpha, \sigma_\beta$ are the clock skew and GPS offset variances which, without loss of generality, are assumed equal for all the PMUs. We set⁴ $\sigma_\alpha = 10^{-2}[\text{rad}]$ assuming a clock accuracy of $\approx 10 \div 30$ ppm [17]; while $\sigma_\beta = 2 \times 10^{-4}[\text{rad}]$, assuming a 50Hz frequency signal and a GPS with $\approx 0.5 \div 1\mu\text{s}$ accuracy [4]. Moreover, having no prior information on the offset and skew biases, we set them to 0. Finally observe that additional correlation terms between active and reactive power can be added. However, in the following we consider the uncorrelated case. Finally, note that the state model has been outlined only for $t \in \mathbb{Z}[0, M]$ assuming k being fixed. At $k+1$ different strategies can be adopted. The simplest one is to re-initialize the filter. However, we underline that we will not discuss on this matter since in the simulation section we will focus on one synchronization window only.

B. Output model

The output model is obtained from the combination of (3) with the PMU measurement model (5). Moreover, from the nominal/predicted demands $\mathbf{p}^*, \mathbf{q}^*$ it is possible to retrieve a feasible point $\mathbf{u}^* = (\mathbf{v}^*, \boldsymbol{\theta}^*)$, used to correctly define the model and, in particular, to compute the matrix $A_{\mathbf{u}^*}$ for the linear approximant. Then, by stacking all the measurement collected at time instant $\tau(k, t)$ in the vector

$$\mathbf{y}(k, t) = \begin{bmatrix} \delta\tilde{\mathbf{v}}(k, t) \\ \delta\tilde{\boldsymbol{\theta}}(k, t) \end{bmatrix} := \begin{bmatrix} \tilde{\mathbf{v}}(k, t) \\ \tilde{\boldsymbol{\theta}}(k, t) \end{bmatrix} - \begin{bmatrix} \mathbf{v}^* \\ \boldsymbol{\theta}^* \end{bmatrix},$$

where $\tilde{\mathbf{v}}(k, t) = [\tilde{v}_1(k, t) \quad \dots \quad \tilde{v}_m(k, t)]^T$, $\tilde{\boldsymbol{\theta}}(k, t) = [\tilde{\theta}_1(k, t) \quad \dots \quad \tilde{\theta}_m(k, t)]^T$, the output model reads as

$$\mathbf{y}(k, t) = H\mathbf{x}(k, t) + \mathbf{w}(k, t), \quad \mathbf{w}(k, t) \sim \mathcal{N}(0, R), \quad (7)$$

²Note that the network' state are the voltages. Hence, picking the power demands as state for the Kalman filter is in contrast with this choice. However, given (3) and the power-demand time series information, the latter seems the most reasonable choice. We stress that this is not restrictive for the following analysis.

³In general, the de-synchronization parameters are of dimension m , where $m \in \mathbb{Z}[0, n]$ is the number of PMUs deployed in the grid.

⁴The value of σ_α largely depends on the type of oscillator used. We assumed PMUs equipped with quartz-crystal oscillator which, due to aging and temperature effects, are characterized by an accuracy $\sim 1 \div 100\text{ppm}$.

Algorithm 1 SASE

Require: P_0, R, H . Initialize $\Sigma(0) = P_0$.

for $t \in \mathbb{Z}[0, M]$ **do** { // Offline computations }
 Compute and store

$$L(t+1) = \Sigma(t)H^T(H\Sigma(t)H^T + R)^{-1} \quad (8a)$$

$$\Sigma(t+1) = (I - L(t+1)H)\Sigma(t) \quad (8b)$$

end for

for $k \in \mathbb{Z}$ **do** { // Online computations }

 Initialize $\hat{\mathbf{x}}(k, 0) = 0$

for $t \in \mathbb{Z}[0, M]$ **do**

$$\hat{\mathbf{x}}(k, t+1) = \hat{\mathbf{x}}(k, t) + L(t+1)(\mathbf{y}(k, t+1) - H\hat{\mathbf{x}}(k, t))$$

end for

end for

where $\mathbf{w}(k, t) := [\mathbf{w}^v(k, t)^T \quad \mathbf{w}^\theta(k, t)^T]^T$,

$$H := \begin{bmatrix} A_{\mathbf{u}^*}^{-1} & \begin{bmatrix} 0 & 0 \\ t\frac{T}{M}I & I \end{bmatrix} \end{bmatrix}.$$

and $R := \text{blkdiag}(\sigma_{\text{pmu}, v}^2 \text{diag}(|\mathbf{v}^*|^2), \sigma_{\text{pmu}, \theta}^2 I)$. It is worth observing that, due to the linear relation (3) between buses' power and network' state, i.e., voltages' magnitude and phase, the de-synchronization enters linearly in the output model (7) without any further approximation.

C. Kalman filter formulation

From (6)–(7), we have at disposal a complete model to run a Kalman filter [16] to simultaneously compute the best linear estimates of system state and de-synchronization parameters. Since in the prescribed case the state vector has no dynamic and there is no process noise, it is convenient to express the Kalman equations in filter form rather than as prediction and correction separately. Algorithm 1 describes what we refer to as *Synchronization Aware State Estimator*, hereafter denoted with SASE. In Algorithm 1 note that, according to the state-space evolution and the periodic synchronization instants, we assume that at every k the filter initial conditions are re-initialized, see Figure 1. Regarding the error covariance matrix $\Sigma(t)$, since it does not depend on the measurements, its evolution can be computed offline and stored for $t \in \mathbb{Z}[0, M]$. Moreover, in view of our modeling choices and, in particular, the absence of state dynamic and process noise, $\Sigma(t)$ is non-increasing, namely we can state the following Lemma whose proof is straightforward thus omitted.

Lemma 2 (Error Covariance matrix evolution): Within two consecutive synchronization instants $k \in \mathbb{Z}_+$, the error covariance matrix Σ (8b), associated to the Kalman filter of Algorithm 1, satisfies $\Sigma(t+1) \leq \Sigma(t)$, $t \in \mathbb{Z}[0, M]$. \square

Finally, according to P_0 , Σ can be partitioned as

$$\Sigma = \begin{bmatrix} \Sigma^p & \Sigma^{pq} & \Sigma^{p\alpha} & \Sigma^{p\beta} \\ \Sigma^{qp} & \Sigma^q & \Sigma^{q\alpha} & \Sigma^{q\beta} \\ \Sigma^{\alpha p} & \Sigma^{\alpha q} & \Sigma^\alpha & \Sigma^{\alpha\beta} \\ \Sigma^{\beta p} & \Sigma^{\beta q} & \Sigma^{\beta\alpha} & \Sigma^\beta \end{bmatrix}.$$

Parameter	Value [units]	Ref.
T	1 [s]	[9]
M	25 [samples]	[12]
σ_p, σ_q	50%	[14]
$\sigma_{\text{pmu},v}, \sigma_{\text{pmu},\theta}$	0.1%, 10^{-3} [rad]	[12]
σ_α	10^{-2} [rad]	[17]
σ_β	2×10^{-4} [rad]	[12]
$\mathbf{v}^*, \boldsymbol{\theta}^*, \mathbf{p}^*, \mathbf{q}^*$	power flow nominal solution	

TABLE I: Parameters used in the simulations

Then, from (3), one has $\begin{bmatrix} \hat{\mathbf{v}} \\ \hat{\boldsymbol{\theta}} \end{bmatrix} = \begin{bmatrix} \mathbf{v}^* \\ \boldsymbol{\theta}^* \end{bmatrix} + A_{\mathbf{u}}^{-1} \begin{bmatrix} \delta \hat{\mathbf{p}} \\ \delta \hat{\mathbf{q}} \end{bmatrix}$, with error covariance matrix given by $\Sigma^{\mathbf{u}} := \begin{bmatrix} \Sigma^v & \Sigma^{v\theta} \\ \Sigma^{v\theta} & \Sigma^\theta \end{bmatrix} = A_{\mathbf{u}^*}^{-1} \begin{bmatrix} \Sigma^p & \Sigma^{pq} \\ \Sigma^{qp} & \Sigma^q \end{bmatrix} A_{\mathbf{u}^*}^{-T}$.

V. SIMULATIONS

Here we compare the proposed SASE algorithm against:

- 1) An online iterative version of the static algorithm presented in [6] (hereafter referred to as *Bayesian Linear State Estimator* – BLSE) which does not assume any synchronization error in the measurements.
- 2) A strategy assuming the presence of an oracle which deterministically tells the CPU the exact desynchronization parameters. Observe that, in the presence of sync error, this is the achievable best thus the strategy is used and referred to as *Ground Truth* – GT.

Differently from the proposed algorithm, both the above cases, i.e., GT and BLSE, return estimates of the voltage quantities $\hat{\mathbf{v}}, \hat{\boldsymbol{\theta}}$ only since either the synchronization parameters are neglected or they are perfectly known.

For consistency, since we compare our approach with the solution proposed in [6], we exploit their same test bed consisting of an 11 kV 50Hz 15 nodes Indian rural distribution feeder [18]. We refer to [6], [18] for additional details.

To test the algorithms we use MATLAB. Regarding the parameters choice, Table I sums up all the values of interest.

We compare the estimation performance in terms of *Average Rooted Mean Squared Error* which, given any two n -dimensional vectors $\mathbf{a}(t), \mathbf{b}(t)$, possibly functions of time, is defined as

$$\text{ARMSE}(\mathbf{a}(t), \mathbf{b}(t), t) := \sqrt{\frac{1}{n} \sum_{h=1}^n \mathbb{E}[|a_h(t) - b_h(t)|^2]}. \quad (9)$$

Observe that, under the assumptions of linear model and correct measurement noise statistic, the Kalman filter error covariance matrix can be exploited since it holds that

$$\text{ARMSE}(t) = \sqrt{\frac{1}{n} \text{Trace}(\Sigma(t))}. \quad (10)$$

However, if either one of the two assumptions above is missing then the equivalence in (10) might not hold. Hence,

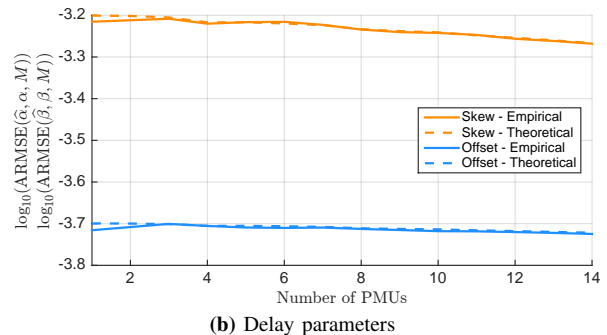
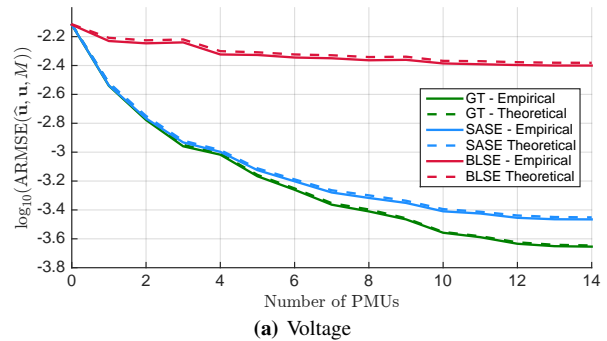


Fig. 2: Empirical $\widehat{\text{ARMSE}}$ (11) and theoretical ARMSE (10), in logarithmic scale, as function of the number of deployed PMUs for $M = 25$.

we also resort to an empirical approximation averaged over $N = 1000$ Monte Carlo runs computed as

$$\widehat{\text{ARMSE}}(\mathbf{a}(t), \mathbf{b}(t), t) = \sqrt{\frac{1}{N} \sum_{i=1}^N \frac{1}{n} \sum_{h=1}^n |a_h(t) - b_h(t)|^2}. \quad (11)$$

In view of the above discussion, it is possible to leverage the comparison between (10) and (11) to perform model qualification. Indeed, $\widehat{\text{ARMSE}}(t) \approx \text{ARMSE}(t)$ means the non-linear measurements statistic is effectively captured by the linear filter built on the approximation. Finally, note that as opposed to SASE and GT, which exploit the true measurements statistic, BLSE ignores the presence of synchronization delay. Hence, to compute the theoretical performance of the filter it is necessary to resort to a modified Riccati equation comprising the correct measurements error statistic. Thus, when we refer to the theoretical values of the ARMSE, we implicitly assume (10) is used where $\Sigma(t)$ is the error covariance matrix for SASE and GT, while for BLSE is the solution of a suitably modified Riccati.

Figure 2 shows the values of $\widehat{\text{ARMSE}}(\cdot, \cdot, M)$ (11) and $\text{ARMSE}(\cdot, \cdot, M)$ (10) for the estimated complex voltage $\hat{\mathbf{u}} = \hat{\mathbf{v}}e^{j\hat{\boldsymbol{\theta}}}$ (Figure 2a) and parameters $\hat{\boldsymbol{\alpha}}, \hat{\boldsymbol{\beta}}$ (Figure 2b) with respect to the true values $\mathbf{u}, \boldsymbol{\alpha}, \boldsymbol{\beta}$ as functions of the number of PMUs deployed in the network when all the $M = 25$ PMU measurements have been processed, i.e., right before a new synchronization instant occurs. Note that the PMUs deployment order affects the performance improvement. However, since the placement policy is out of the scope of the paper, we resort to the greedy algorithm proposed in [6] which we refer the reader to.

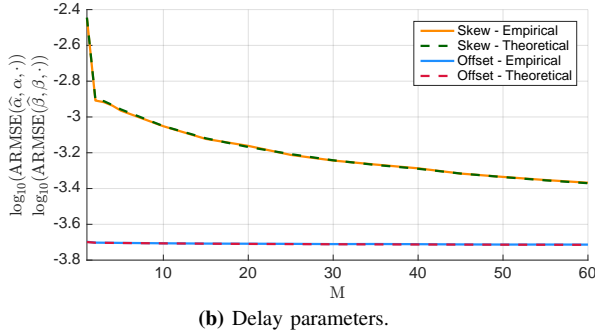
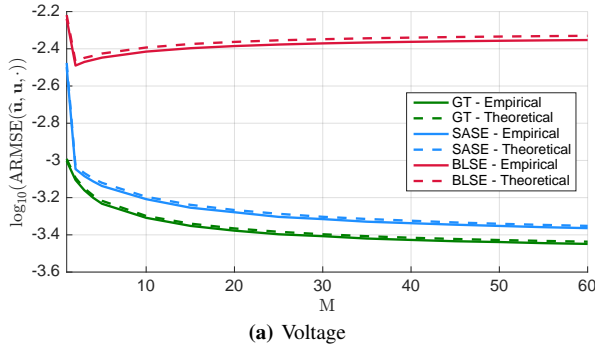


Fig. 3: Empirical $\widehat{\text{ARMSE}}$ (11) and theoretical ARMSE (10), in logarithmic scale, as function of the number of collected PMU measurements M , for 8 PMUs deployed in the network. $M \in [0, 60]$ to consider the PMU reporting rates for both the 50Hz and 60Hz standards.

From Figure 2a, it is interesting to note that i) the proposed SASE approach behaves almost indistinguishable from the GT while ii) the unmodeled synchronization error clearly deteriorates the BLSE, whose performance achieves, at best, $\approx 30\%$ improvement. Conversely, the SASE performance with just one PMU improves of $\approx 60\%$. Thus, at worst, it performs twice as better as the BLSE with the full set of PMUs deployed. Regarding the de-synchronization, Figure 2b shows that the estimation performance does not clearly improve for increasing number of PMUs deployed. This can be expected since the synchronization error parameters of different PMUs have been assumed uncorrelated. Finally, note that in both Figure 2a and 2b, theoretical and empirical curves almost perfectly coincide, validating the goodness of the prescribed linear approximation. We remind this holds for parameters values as in Table I.

Figure 3 shows the performance for different PMU reporting rate. That is for a fixed number of PMUs, the Figure shows the evolution of the $\widehat{\text{ARMSE}}(\cdot, \cdot, \cdot)$ (11) and of the $\text{ARMSE}(\cdot, \cdot, \cdot)$ (10) as functions of the number of collected PMU measurements M . Figure 3a confirms the good behavior of SASE compared with GT. Conversely, as time passes, the BLSE does not improve since it has no clue about the presence of the delay. Figure 3b supports this claim. Indeed, since the estimated skew improves for increasing M , the SASE is able to compensate for it. Finally, Figure 3b shows that the offset does not improve with M . This is an intrinsic modeling problem due to the fact that offset and power demand happen to be linearly dependent.

VI. CONCLUSIONS

In this paper we addressed the problem of state estimation in power systems. We considered the presence of PMUs de-synchronization and analyzed the problem of simultaneous state and synchronization error parameters estimation. By casting the problem in a Bayesian framework while resorting to a novel linear approximation for the power flow equations, we proposed a Kalman filtering procedure to achieve the purpose. Interestingly, it is shown how the presence of synchronization error easily misleads the estimator if the measurements model does not properly account for it.

REFERENCES

- [1] A. Abur and A. G. Exposito, *Power system state estimation: theory and implementation*. CRC press, 2004.
- [2] F. C. Schweppe *et al.*, "Power system static-state estimation, part i-iii," *IEEE Transactions on Power Apparatus and Systems*, no. 1, pp. 120–130, 1970.
- [3] G. T. Heydt, "The next generation of power distribution systems," *IEEE Transactions on Smart Grid*, vol. 1, no. 3, pp. 225–235, 2010.
- [4] [Online]. Available: <http://www.arbiter.com/files/product-attachments/1133a.pdf>
- [5] A. Phadke, J. Thorp, and K. Karimi, "State estimation with phasor measurements," *IEEE Transactions on Power Systems*, vol. 1, no. 1, pp. 233–238, 1986.
- [6] L. Schenato, G. Barchi, D. Macii, R. Arghandeh, K. Poolla, and A. Von Meier, "Bayesian linear state estimation using smart meters and pmus measurements in distribution grids," in *Smart Grid Communications (SmartGridComm), 2014 IEEE International Conference on*. IEEE, 2014, pp. 572–577.
- [7] G. Barchi, D. Fontanelli, D. Macii, and D. Petri, "On the accuracy of phasor angle measurements in power networks," *Instrumentation and Measurement, IEEE Transactions on*, vol. 64, no. 5, pp. 1129–1139, 2015.
- [8] S. Bolognani, R. Carli, and M. Todescato, "State estimation in power distribution networks with poorly synchronized measurements," December 2014, pp. 2579–2584.
- [9] P. Yang, Z. Tan, A. Wiesel, and A. Nehorai, "Power system state estimation using pmus with imperfect synchronization," *IEEE Transactions on power Systems*, vol. 28, no. 4, pp. 4162–4172, 2013.
- [10] J. A. Bazerque, U. Ribeiro, and J. Costa, "Synchronization of phasor measurement units and its error propagation to state estimators," in *Innovative Smart Grid Technologies Latin America (ISGT LATAM), 2015 IEEE PES*. IEEE, 2015, pp. 508–513.
- [11] S. Bolognani and F. Drfler, "Fast power system analysis via implicit linearization of the power flow manifold," in *2015 53rd Annual Allerton Conference on Communication, Control, and Computing (Allerton)*, Sept 2015, pp. 402–409.
- [12] "Ieee standard for synchrophasor measurements for power systems," *IEEE Std. C37.118.1*, 2011.
- [13] S. V. Dhople, S. S. Guggilam, and Y. C. Chen, "Linear approximations to ac power flow in rectangular coordinates," in *2015 53rd Annual Allerton Conference on Communication, Control, and Computing (Allerton)*, Sept 2015, pp. 211–217.
- [14] R. Sevljan and R. Rajagopal, "Short term electricity load forecasting on varying levels of aggregation," *arXiv preprint arXiv:1404.0058*, 2014, submitted to Power Systems, IEEE Transactions on.
- [15] A. Borghetti, C. Nucci, M. Paolone, G. Ciappi, and A. Solari, "Synchronized phasors monitoring during the islanding maneuver of an active distribution network," *IEEE Transactions on Smart Grid*, vol. 2, no. 1, pp. 82–91, Mar. 2011.
- [16] R. E. Kalman, "A new approach to linear filtering and prediction problems," *Journal of basic Engineering*, vol. 82, no. 1, pp. 35–45, 1960.
- [17] J. R. Vig, "Quartz crystal resonators and oscillators for frequency control and timing applications. a tutorial," *NASA STU/Recon Technical Report N*, vol. 95, 1994.
- [18] D. Das, D. Kothari, and A. Kalam, "Simple and efficient method for load flow solution of radial distribution networks," *International Journal of Electrical Power & Energy Systems*, vol. 17, no. 5, pp. 335–346, 1995.